



Defence Research and
Development Canada

Recherche et développement
pour la défense Canada



Wind tunnel tests on two-dimensional air intakes at DRDC Valcartier

*D. Corriveau
R. Pimentel
DRDC Valcartier*

Defence R&D Canada – Valcartier

Technical Memorandum

DRDC Valcartier TM 2008-116

April 2009

Canada

Wind tunnel tests on two-dimensional air intakes at DRDC Valcartier

D. Corriveau
R. Pimentel
DRDC Valcartier

Defence R&D Canada – Valcartier

Technical Memorandum
DRDC Valcartier TM 2008-116
April 2009

Authors

D. Corriveau, R. Pimentel
Defence Scientists

Approved by

Alexandre Jouan
Head, Precision Weapons Section

Approved for release by

Christian Carrier
Chief Scientist

Abstract

An increasing interest in ramjet propulsion for tactical supersonic missiles has been observed worldwide recently, due to the improved performance it provides in terms of range and speed compared to solid propellant rocket propulsion. DRDC Valcartier in Canada and TNO Defence, Security and Safety in the Netherlands are currently working jointly to improve their capacity to numerically predict the internal performance of ramjet powered missiles. Air intakes are employed on several operational cruise missiles that use ramjet airbreathing propulsion during the supersonic cruise flight phase. It is recognized that the operation of airbreathing missiles is strongly dependent on the efficiency of their air intake systems.

Accurate experimental data on the performance parameters of ramjet air intakes at different angles of attack during on- and off-design operation are required in order to verify the accuracy of numerical predictions. However, the quantity and quality of experimental data on air intake performance available in the open literature are very limited. Therefore, it was decided to investigate the possibility of performing air intake performance measurements in the trisonic wind tunnel at DRDC Valcartier to generate additional experimental data for comparison with numerical simulations. This memorandum describes possible procedures and instrumentation that would be required to test ramjet air intakes in the DRDC Valcartier trisonic wind tunnel.

Résumé

On observe dans le monde une augmentation de l'intérêt envers les statoréacteurs pour la propulsion des missiles supersoniques en raison de leurs meilleures performances au point de vue portée et vitesse comparativement à la propulsion avec des propergols solides. RDRC Valcartier au Canada et TNO Defence, Security and Safety aux Pays-Bas travaillent présentement conjointement afin d'améliorer leur capacité à prédire numériquement la performance des statoréacteurs. Les entrées d'air sont utilisées pour divers missiles de croisière avec propulsion à l'aspiration d'air pendant la phase de vol supersonique.

Des données précises sur la performance des prises d'air pour statoréacteurs sont requises à angle d'attaque et en condition non standard afin de vérifier la précision des prédictions numériques. Cependant, la quantité et la qualité des données expérimentales sur les prises d'air disponibles dans la littérature ouverte sont assez limitées. On a donc décidé d'envisager la possibilité d'effectuer des mesures de la performance des prises d'air dans la soufflerie trisonique de RDRC Valcartier de manière à générer des données expérimentales additionnelles pour fins de comparaison avec les simulations numériques. Ce mémorandum décrit les procédures possibles et l'instrumentation nécessaires pour la réalisation des essais éventuels à la soufflerie trisonique de RDRC Valcartier sur les entrées d'air pour statoréacteurs.

This page intentionally left blank.

Executive summary

An increasing interest in ramjet propulsion for tactical supersonic missiles has been observed due to its improved performance in terms of range and speed compared to solid propellant rocket propulsion. DRDC Valcartier in Canada and TNO Defence, Security and Safety in the Netherlands are currently working jointly to improve their capacity to numerically predict the performance of ramjet powered missiles. Air intakes are employed on several operational cruise missiles that use ramjet airbreathing propulsion during the supersonic cruise flight phase. It is recognized that the operation of airbreathing missiles is strongly dependent on the efficiency of their air intake systems.

Accurate experimental data on ramjet air intake performance at different angles of attack during on- and off-design operation are required in order to verify the accuracy of numerical models. However, the open literature survey revealed that the amount of data available to properly validate performance prediction codes applied to ramjet engines was very limited. Therefore, it was decided to investigate the possibility of performing air intake performance measurements in the trisonic wind tunnel at DRDC Valcartier to generate additional experimental data for comparison with numerical simulations.

This memorandum presents the procedures and instrumentation needed to test supersonic air intakes in the DRDC Valcartier trisonic wind tunnel. A series of reports from Volvo Flygmotor AB concerning 2-D air inlets for use on cruise missiles using ramjet airbreathing propulsion were considered the most suitable for our studies. The reports present several results on different configurations of 2-D supersonic air inlets both in isolation and mounted on a missile body, as well as detailed drawings for the construction of a wind tunnel model. For the tests at DRDC Valcartier the research efforts will focus on the main air intake performance parameters. The air intake will be studied in isolation in order to eliminate the complexities related to the influence of the missile forebody.

The Volvo reports include data on the air intake performance parameters, such as pressure recovery and mass flow rate measurements as a function of Mach number, angle of attack and intake backpressure. Pressure recovery data are also presented for various bleed flow rates. For the tests to be carried out in the DRDC Valcartier trisonic wind tunnel, static pressure taps along the compression surface and the cowl could gather more information about flow physics which is not provided in the Volvo reports. Also, no flow diagnostics such as Schlieren photography, particle image velocimetry or oil dots were presented. Flow visualization techniques could be considered in the DRDC Valcartier experiment to complement the Volvo database and provide the information on shock location and boundary layer separation necessary for numerical validation.

Corriveau, D., Pimentel, R., 2009. Procedures for Wind Tunnel Tests on Two-Dimensional Air Intakes at DRDC Valcartier. DRDC Valcartier TM 2008-116; Defence R&D Canada – Valcartier.

Sommaire

Une augmentation de l'intérêt pour les missiles supersoniques tactiques propulsés par des statoréacteurs a été observée en raison de leurs performances supérieures au point de vue portée et vitesse si on compare avec les missiles propulsés par propergols solides. RDDC Valcartier au Canada et TNO Defence, Security and Safety au Pays-Bas coopèrent pour améliorer ses capacités de prédiction numérique de la performance des missiles propulsés par statoréacteurs. Les entrées d'air sont employées dans plusieurs missiles de croisière qu'utilisent des statoréacteurs durant sa phase de vol supersonique. Il est reconnu que l'utilisation de tels missiles est fortement dépendante de l'efficacité des systèmes d'entrées d'air.

Des données expérimentales précises sur la performance des entrées d'air par des statoréacteurs à différents angles d'attaque et conditions d'opération sont requises pour la vérification de la précision de modèles numériques. Cependant, on a noté dans la littérature ouverte que la quantité des données expérimentales pour valider adéquatement les logiciels de prédiction de la performance des moteurs aux statoréacteurs est très limitée. On a donc décidé d'étudier la possibilité de procéder à des essais à la soufflerie trisonique de RDDC Valcartier pour générer les données expérimentales nécessaires à la validation des simulations numériques.

Ce mémorandum présente les procédures et l'instrumentation requises pour réaliser des essais sur les entrées d'air supersoniques à la soufflerie trisonique de RDDC Valcartier. Une série de rapports de la compagnie VOLVO Flygmotor AB sur les entrées d'air rectangulaires utilisées sur les statoréacteurs a semblé être plus adéquat pour nos études. Ces rapports présentent différents résultats expérimentaux sur différentes configurations d'entrées d'air rectangulaires en isolation et assemblées sur le boîtier de missiles. Pour les essais à RDDC Valcartier, l'effort de la recherche peut être concentré sur les performances principales des entrées d'air. L'étude de celles-ci de façon isolée permet d'éliminer les complexités causées par l'influence du boîtier du missile sur elles-mêmes.

Les rapports de VOLVO présentent plusieurs paramètres de performance des entrées d'air, tels que la récupération de pression et le débit massique en fonction du nombre de Mach, de l'angle d'attaque et de la contrepression. Les données de récupération de la pression sont aussi présentées pour différents taux d'aspiration de la couche limite sur la surface de compression. Pour des essais éventuels à la soufflerie trisonique de RDDC Valcartier, les mesures de la pression statique sur la surface de compression et le capot peuvent apporter des informations additionnelles sur la physique de l'écoulement qui sont absentes dans les rapports de VOLVO. En outre, aucune technique de diagnostic d'écoulement telle que Schlieren, PIV goutte d'huile est présentée. De telles techniques de visualisation d'écoulement peuvent être envisagées pour compléter les données expérimentales présentées dans les rapports de VOLVO et fournir des informations sur la localisation des ondes de choc et de la séparation de la couche limite qui sont nécessaires à la validation des simulations numériques.

Corriveau, D., Pimentel, R., 2009. Procedures for Wind Tunnel Tests on Two-Dimensional Air Intakes at DRDC Valcartier. DRDC Valcartier TM 2008-116; R & D pour la defense Canada - Valcartier.

Table of contents

Abstract	i
Résumé	i
Executive summary	iii
Sommaire	iv
Table of contents	v
List of figures	vi
List of tables	vii
1 Introduction.....	1
2 Intake Configuration Selection	2
3 Model Installation.....	4
4 Intake Backpressure Control and Mass Flow Rate Measurements.....	5
4.1 Intake Backpressure Control	6
4.2 Mass Flow Rate Measuring Techniques.....	8
4.2.1 Duct-based Mass Flow Rate Estimation	8
4.2.2 Debitmetre.....	9
4.2.3 Chocked Valve.....	10
4.3 Mass Flow Rate	10
4.4 Calibration Procedure.....	11
4.4.1 Calibration Rig.....	11
4.4.2 Discharge Coefficient.....	14
4.5 Flow cell exit area calculation.....	15
5 Total Pressure Recovery Measurements.....	17
6 Air Intake Instrumentation.....	19
6.1 Surface Static Pressure Measurements	19
6.2 Pitot Tube Rake	21
6.3 Boundary Layer Control and Survey.....	23
6.4 Oil Dots Visualization	24
6.5 PIV Measurements	25
6.6 Schlieren Technique	26
7 Tentative Test Matrix.....	28
8 Conclusions.....	31
9 References.....	33
List of symbols/abbreviations/acronyms/initialisms	35
Distribution list.....	37

List of figures

Figure 1: Air intake cross-section.....	2
Figure 2: Test configuration used by VOLVO.....	3
Figure 3: Pitot intake set-up for experimental tests in isolation.....	4
Figure 4: Operating modes of ramjet air intakes.....	5
Figure 5: Flow cell equipped with a Pitot rake at the inlet and a conical valve.....	6
Figure 6: Conical valve used to control intake mass flow rate.....	6
Figure 7: Air intake with a prismatic valve used to control the mass flow rate.....	7
Figure 8: Debitmetre.....	9
Figure 9: Actual capture area.....	10
Figure 10: Flow cell calibration rig.....	12
Figure 11: Flow cell calibration rig for DRDC Valcartier trisonic wind tunnel.....	13
Figure 12: Valve on the wind tunnel reservoir.....	13
Figure 13: Bellmouth nomenclature.....	15
Figure 14: Nomenclature for the cell exit.....	15
Figure 15: Ramjet engine schematic.....	17
Figure 16: Pitot tube rake.....	22
Figure 17: 2-D Pitot tube rakes.....	22
Figure 18: Boundary layer bridging across an isentropic ramp.....	23
Figure 19: Boundary layer probe traverse set-up.....	24
Figure 20: PIV set-up for air intake tests.....	25
Figure 21: Typical Schlieren arrangement – The Z-Type 2-mirrors.....	26
Figure 22: Typical Schlieren arrangement – Single mirror coincident system.....	27

List of tables

Table 1: Field Definitions..... 28

Table 2: Test Matrix – Mach Number 2.5..... 28

Table 3: Test Matrix – Mach Number 2.5..... 29

Table 4: Test Matrix – Mach Number 3.0..... 30

This page intentionally left blank.

1 Introduction

A review of the studies in the open literature on supersonic air intakes revealed that the amount of data available to validate performance prediction codes in this field is very limited. Furthermore, most studies provide only limited details concerning model geometry and do not permit the complete reproduction of test models for experiments or the generation of suitable meshes necessary for numerical calculations.

To fill this gap in the open literature, it was decided to perform a preliminary study on the possibility of performing air intake tests in the trisonic wind tunnel at DRDC Valcartier and to improve our experimental database on air intake performance parameters. Given the limited experience in experimental testing and design of air intakes at DRDC Valcartier, the favoured initial approach would consist of reproducing wind tunnel tests on existing configurations for which the geometric parameters and performance results are readily available. In addition to reproducing the experimental data already available, new measurements could be performed in order to better understand the intake's performance and facilitate further comparisons with the numerical results.

The purpose of this report is to identify the requirements to perform experimental tests on a rectangular ramjet air intake in the trisonic wind tunnel at DRDC Valcartier and to study its internal performance parameters, such as pressure recovery, flow distortion, flow stability and captured mass flow rate.

The experimental data thus obtained would be used to validate performance predictions from Navier-Stokes codes, such as Fluent[®]. Both the experimental and validated numerical results on 2-D inlet performance will form a database for the semi-empirical code DRCORE. DRCORE is being developed by DRDC Valcartier and TNO in order to predict the performance of fully integrated ramjet powered missiles [1]. Finally, by performing ramjet air intake tests, DRDC Valcartier would improve its expertise in this field and lay the groundwork for new research opportunities in the future.

2 Intake Configuration Selection

From the different documents gathered during the literature survey, a series of reports from VOLVO Flygmotor AB, concerning 2-D air intakes for use on cruise missiles using ramjet airbreathing propulsion, appeared to be the most suitable for our purposes. The combustion and aerodynamics department of VOLVO tested several configurations of 2-D supersonic air intakes both in isolation and mounted on a missile body. For some of the configurations, detailed drawings were provided so that a similar air intake wind tunnel model could be manufactured at DRDC Valcartier.

The configuration chosen consists of a 2-D intake with a design Mach number of 2.5. The internal cowl lip angle is 12 deg. Inlet ramp boundary layer bleed is achieved through a bleed insert. Fig. 1 presents a cross-sectional view of the VOLVO's intake, where the main parts of the model can be seen [2]. More details on the design of this model can be found in [3].

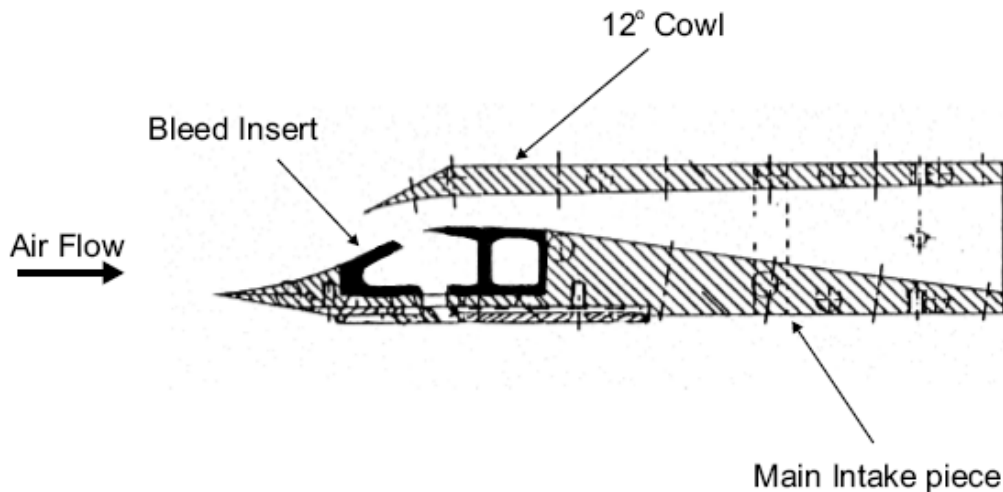


Figure 1: Air intake cross-section.

The geometry of VOLVO's air intake could be extracted reasonably well from the information available in their reports. The freestream conditions of VOLVO's experiments, concerning the two similar rectangular air intakes mounted on a missile body, are:

- Mach 2.22, 2.45 and 2.90
- Angles-of-attack (AoA) between -2.5 deg and 5deg
- Reynolds number based on inlet lip height roughly between 0.70×10^6 and 0.85×10^6

This particular inlet was designed to be used in combination with a second one 90 deg apart as shown in Fig. 2 [4]. However, the model was also tested in isolation at zero AoA for Mach numbers between 2 and 4.

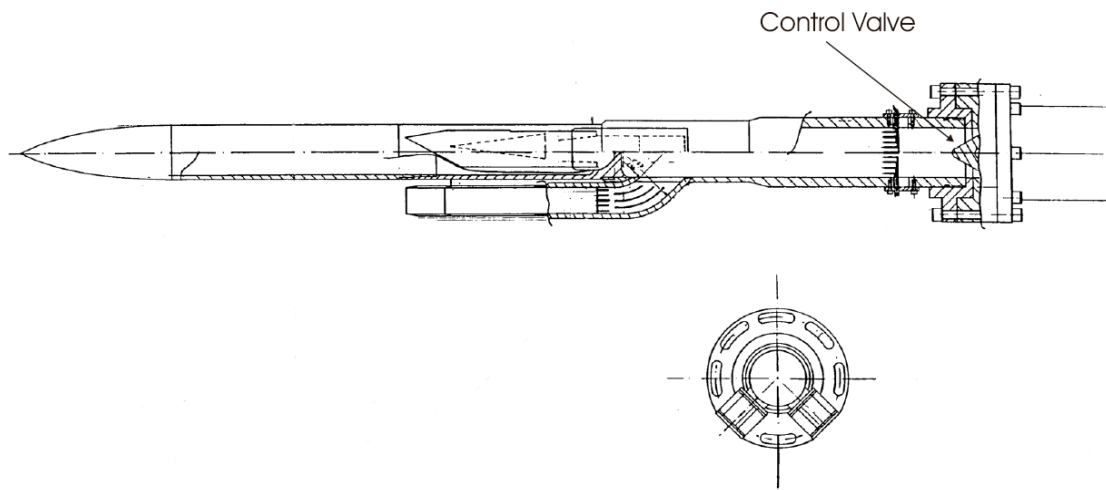


Figure 2: Test configuration used by VOLVO.

The VOLVO report about this particular intake includes a significant amount of data pertaining to overall internal performance parameters, such as pressure recovery and mass flow rate measurements as a function of Mach number, AoA and intake backpressure. Pressure recovery data are also presented for various bleed flow rates. Unfortunately, the report lacks of detailed static pressure distribution along the compression surface or the cowl, for instance. Furthermore, no flow diagnostics, such as Schlieren photography, PIV, oil dots or other techniques are presented which would help in identifying shock locations, boundary layer separation, etc. and thus permit a better picture of the flow physics associated with the air intake.

In order to evaluate the prediction capability of general purpose Computational Fluid Dynamics (CFD) codes on internal aerodynamics of air intake, a clearer picture of the flow physics is certainly highly desirable. Therefore, the possibility of performing complimentary wind tunnel tests at DRDC trisonic wind tunnel on the VOLVO air intake should be considered seriously. A description of additional measurements that could be performed on the VOLVO air intake is presented in Section 6.

3 Model Installation

Several tests carried out by VOLVO were related to air intakes fully integrated with the missile body. They used this configuration in order to investigate the performance of the twin inlet side dump connectors to the combustor and to take into account the influence of the missile forebody on the intake performance.

To constrain our research efforts, the influence of the missile forebody should be eliminated to test the air intake in isolation. In this case, it would only be necessary to have a model that extends up to the subsonic diffuser end. Hence, the size of the test model could be made larger, while still fitting in the limited space available in the DRDC Valcartier trisonic wind tunnel test section.

The use of a larger model results in higher Reynolds number based on inlet height. This is highly desirable as the trisonic wind tunnel operates at very low pressures and thus the resulting Reynolds numbers per unit length are relatively small. Additional discussions on the Reynolds numbers to be expected in the DRDC wind tunnel and the effect on the intake performance are provided further in Section 6.3.

Alternatively, if the model is truncated but its scale is not increased, it would be possible to perform test at higher incidences before the tip or the leading edge of the model reaches the Mach rhombus boundary. Our final choice for the size of our air intake test model is twice the size of VOLVO's air intake. Argumentation for this choice can also be found in Section 6.3.

In order to mimic different operation conditions in the combustion chamber, variable backpressures could be generated using a prismatic valve at the end of the intake model. An example of such arrangement can be seen in Fig. 3, which depicts an experimental setup for a subsonic Pitot intake tested in isolation. The conical valve used to simulate the combustor could be seen on the right end of the figure.

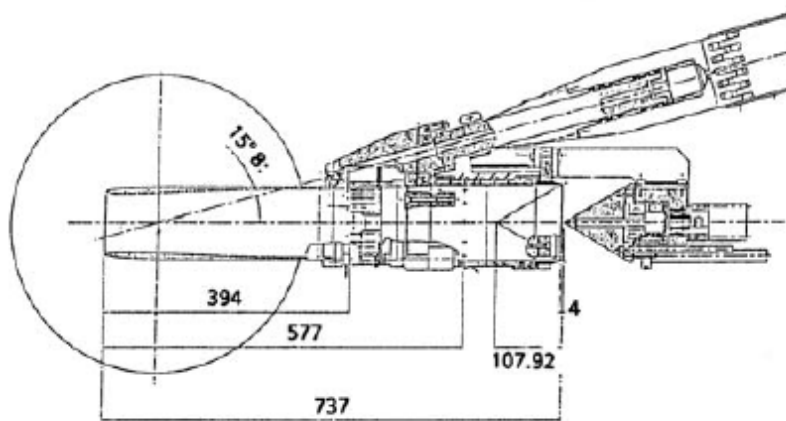


Figure 3: Pitot intake set-up for experimental tests in isolation.

4 Intake Backpressure Control and Mass Flow Rate Measurements

The purpose of an air intake consists, among other things, of allowing a suitable mass of air in the combustion chamber required by the combustion process. As such, the mass flow rate through the intake constitutes an important parameter that must be measured with high accuracy.

As pointed out by Seddon and Goldsmith [5], ideally, measurement errors of the order of $\pm 0.5\%$ are desired. However, due to the difficulties associated with this type of measurements, in practice error of $\pm 1\%$ on the mass flow rate would be considered acceptable. Furthermore, in non-uniform flows the magnitude of such errors could reach values as high as $\pm 10\%$.

As illustrated in Fig. 4, the ramjet air intakes can work in several operating modes namely the subcritical, critical and supercritical modes [6]. The operating mode is determined by the throttling of the ramjet combustor and by the conditions of the flow upstream of the air intake (Mach number, angle-of-attack, flow uniformity, etc.).

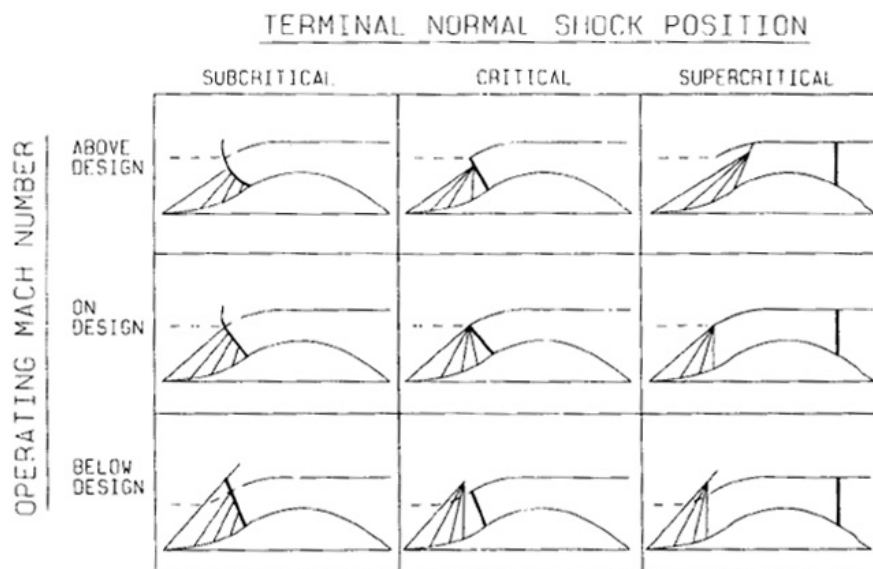


Figure 4: Operating modes of ramjet air intakes.

The intake backpressure that is determined by the combustion process in a real application needs to be controlled to permit the investigation of the air intake performance as function of the operating mode. The ways to simulate different operating conditions of the combustor chamber is the subject of the next sub-section.

4.1 Intake Backpressure Control

To simulate the presence of a combustor and obtain the desired backpressure in the intake, a conical plug located downstream of the Pitot tube rake is often used. Details of a conical valve for such a purpose can be seen in Fig. 5 and in Fig. 6 [7].

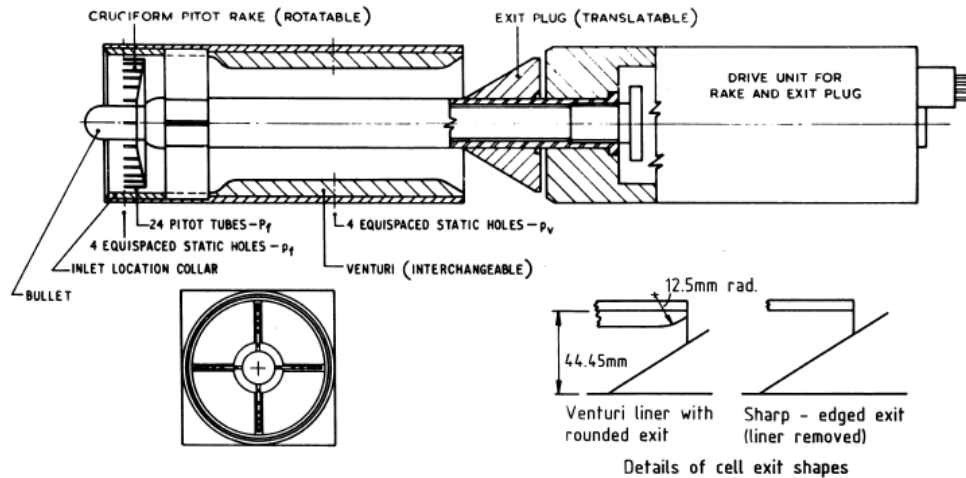


Figure 5: Flow cell equipped with a Pitot rake at the inlet and a conical valve.

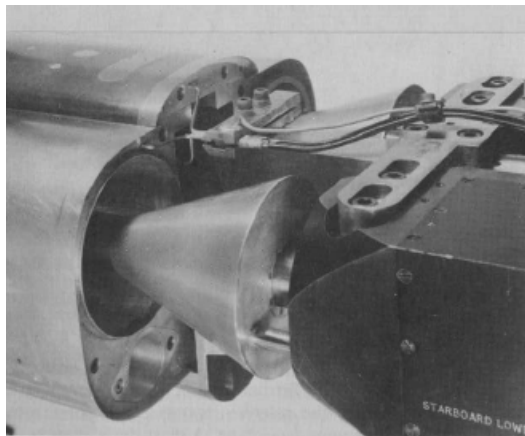


Figure 6: Conical valve used to control intake mass flow rate.

Fig. 3 shown previously gives an example of how the conical valve might be attached on an air intake test setup. The valve can either be translated using a stepper motor or adjusted manually. In a continuously running wind tunnel the former option would be preferable, since it allows the testing for several intake backpressures without interrupting the wind tunnel tests campaign to

change valve settings. On the other hand, in an intermittent facility this advantage is partly lost and the extra cost associated with a motor driven valve may not be worthwhile.

In the case of the DRDC Valcartier Wind Tunnel, an intermittent facility, the disadvantage of using a manually adjustable valve for tests is the extra time required to open the test section and manually adjust the valve. Furthermore, for safety reasons, at the DRDC Valcartier wind tunnel facility, the vacuum tank at the downstream end of the test section must be filled with air to 80% of ambient pressure when the test section is open. This filling of the vacuum tank and emptying of the tank prior to the next test would add extra time when a manually adjustable valve is used. Despite the advantages of using an automatic valve previously mentioned, for sake of simplicity on fabrication, operation and integration to the wind tunnel test section, a manually adjustable valve would be the best trade-off for the tests to be carried out in the DRDC Valcartier trisonic wind tunnel. The valve should be located at some length downstream of the subsonic diffuser and aligned with the inlet longitudinal axis.

The simplest configuration for the adjustable valve would be conical, as previously shown in Fig. 5 and Fig. 6, or prismatic shapes. However, since the interest of the present study is on 2-D air intake, the use of a conical valve would require a transition piece to turn the rectangular cross-section of the air intake into a circular one. This adds to the complexity in several ways. Obviously a transition piece should be designed to minimise flow perturbations. Furthermore, with a conical valve possibly two Pitot tube rakes would have to be used. A rectangular Pitot tube rake would be needed at the end of the subsonic diffuser to calculate the pressure recovery and the flow distortion. These data would eventually be used for comparison with the numerical predictions. The second Pitot tube rake required would be located in the circular cross-section duct upstream from the conical valve. It would be needed to obtain an accurate measure of the total pressure required for the mass flow rate calculations.

An alternative to the conical valve would be the use of a prismatic valve with a rectangular projected area. Such valve geometry was used by Wollett & Connors [8] to control the backpressure in a 2-D air intake tested in a wind tunnel. The configuration they used is shown in Fig. 7.

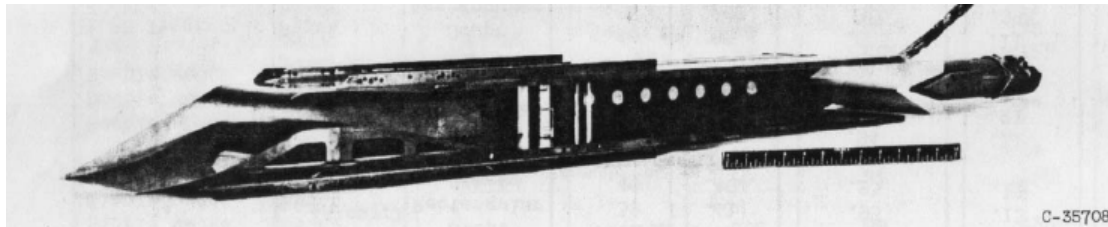


Figure 7: Air intake with a prismatic valve used to control the mass flow rate.

The advantage of using a prismatic valve is that it simplifies greatly the manufacturing of the wind tunnel model. First, no transition piece is required at the end of the subsonic diffuser as the valve has the same projected cross-sectional shape as the air intake. Furthermore, the same Pitot tube rake can be used to determine the total pressure recovery, flow distortion and mass flow rate.

For the ramjet air intake tests to be performed at DRDC Valcartier, the use of a prismatic valve for intake backpressure control would be the best choice in order to minimize complexity on design, fabrication and integration of the model to the test section.

4.2 Mass Flow Rate Measuring Techniques

4.2.1 Duct-based Mass Flow Rate Estimation

Several techniques can be used to determine the mass flow rate through an air intake. The simplest one consists of using the combination of total pressure measurements obtained from a Pitot tube rake and duct wall static pressure measurements at a location where the duct cross-sectional area is known. Usually, this rake is also used to determine other internal performance parameters, such as the flow distortion and the pressure recovery of the air intake. These pressure measurements yield the local Mach number M :

$$M = \sqrt{\frac{2}{\gamma - 1} \left[\left(\frac{P_{0\infty}}{P_B} \right)^{\frac{\gamma - 1}{\gamma}} - 1 \right]} \quad (1)$$

The dimensionless mass flow rate from Fliegner's number requires a total temperature T_0 reading to calculate the mass flow rate, as shown in Eq. 2.

$$\frac{m \sqrt{T_0}}{A P_0} = \sqrt{\frac{\gamma}{R}} \frac{M}{\left[1 + \frac{\gamma - 1}{2} M^2 \right]^{\frac{\gamma + 1}{2(\gamma - 1)}}} \quad (2)$$

The calculation of mass flow rate by this method has two disadvantages. The first one concerns the determination of the mean total pressure which may be not accurate enough due to the presence of flow non-uniformity as well as the limited spatial resolution that can be obtained in the wall boundary layer region. The accuracy can probably be made acceptable by using enough total pressure probes, evenly distributed over the entire duct cross-section.

The second disadvantage occurs for the near subcritical intake operational modes corresponding with deep wedge insertion depths to provide higher backpressures. These operational modes correspond to lower mean Mach numbers in the duct, which implies relatively small differences between static and total pressures. The difference between mean static pressure and mean total pressure determines the duct Mach number (see Eq. 1). When this difference becomes small, the inaccuracies of the pressure measurements may cause inaccurate values of the duct Mach number and therefore also inaccurate estimations of the intake mass flow rate. Therefore, special attention should be taken during the selection of the most suitable pressure sensors for the experiments.

4.2.2 Debitmetre

An accurate method to determine the mass flow rate is to use a settling chamber in series with a sonic throat. Such apparatus is called a debitmetre and is shown in Fig. 8. The settling chamber is equipped with static taps and thermocouples. The Mach number in the settling chamber M_s can be obtained since A_s / A^* is known. A_s is the cross-sectional area of the settling chamber and A^* is the area of the choked nozzle. Thus, using Fliegner's number (Eq. 2), the mass flow rate can be calculated. By doing so, the assumption of the total pressure being very close to the measured static pressure is made. The total pressure is required to estimate the mass flow rate according to Eq. 1 and Eq. 2.

The mass flow rate can be estimated in an alternative way by using the relation between mass flow rate, total pressure, sonic throat area and characteristic velocity:

$$\dot{m} = \frac{P_0 \cdot A^*}{c^*} \quad (3)$$

Where the characteristic velocity c^* is defined as:

$$c^* = \frac{\sqrt{\gamma \cdot R_{air} \cdot T_0}}{\gamma \cdot \sqrt{\left(\frac{2}{\gamma+1}\right)^{\frac{\gamma+1}{\gamma-1}}}} \quad (4)$$

Corrections in the form of a discharge coefficient are required for both mass flow rate estimation methods to take into account the throat curvature and the boundary layer on the throat surface.

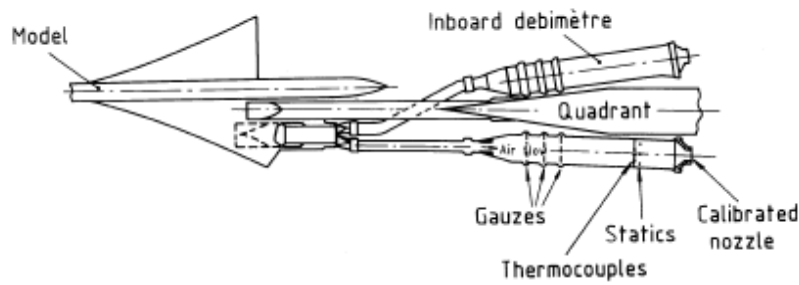


Figure 8: Debitmetre.

4.2.3 Choked Valve

The use of a flowmeter incorporating a settling chamber together with a sonic throat is not always possible in an experimental facility due to space limitations. A valid alternative to a debitmetre can be obtained if a valve is present to control the flow. In such cases, the valve used to adjust the mass flow rate can be also used as a sonic throat, Eq. 3.

This method has two disadvantages. The first one is similar to the first disadvantage mentioned for the duct-based mass flow estimation technique (see section 4.2.1) and is related to the challenge of obtaining a good average of the total pressure in non-uniform flows and boundary layer flow along the duct walls. The accuracy can probably be made acceptable by using enough total pressure probes that are evenly distributed over the entire duct cross-section.

The second disadvantage is also related to flow non-uniformity and the presence of boundary layers. The flow upstream of the wedge will be distorted to a certain extent, especially for the supercritical operational modes with the normal shock system positioned deep inside the intake. This affects the effective throat area that is usually determined by conducting calibration experiments that yield discharge coefficients with which the geometrical throat area must be multiplied in order to obtain effective throat areas. For homogeneous duct flows and a given sonic throat geometry (e.g. conical or prismatic), one can set up calibration experiments that yield discharge coefficients that are a function of the valve insertion depth. However during the actual ramjet air intake tests, the flow in the duct will be inhomogeneous and the flow will differ as function of many variables (freestream Mach number, angle-of-attack, bleed system setting and wedge insertion depth). The discharge coefficients to be applied for accurate mass flow rate estimations depend on all these variables. For the cases where this technique is used, discharge coefficients derived from calibration experiments that are based on homogeneous duct flow may therefore not be accurate enough for the actual ramjet air intake tests and thus should be investigated.

4.3 Mass Flow Rate

In presenting results related to air intakes, the dimensionless flow ratio or capture area ratio A_∞ / A_c is often quoted instead of the mass flow rate. A_c is the geometrically determined area corresponding with the maximum amount of captured air, occurring during on or above design and (super)critical intake operational conditions whereas A_∞ is the actual capture area.

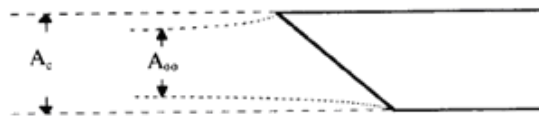


Figure 9: Actual capture area.

For choked exit conditions, the flow ratio is given by

$$\frac{\dot{A}_\infty}{A_c} = \frac{P_{0f}}{P_{0\infty}} \cdot \frac{\dot{A}_e}{A_c} \cdot \left(\frac{A}{A^*} \right)_\infty \quad (5)$$

In this equation, P_{0f} is the average pressure obtained from the Pitot tube rake. Details on the proper way to calculate P_{0f} are given in Section 5. A_e is the valve sonic throat area. In calculating the dimensionless flow ratio, the choked throat area A_e must be the effective area $A_{e, effective}$ and not the geometric area $A_{e, geometric}$ in order to take into account the presence of surface boundary layers and flow non-uniformity. The effective area can be obtained through a calibration process described in the following section.

4.4 Calibration Procedure

For the sonic throat-based mass flow rate estimation techniques (see Sections 4.2.2 and 4.2.3), the estimations must be calibrated in order to obtain the effective sonic throat area which by definition differs from the chosen geometrical throat area. The duct-based mass flow rate estimation technique does not require calibration since it is based on the known duct area.

4.4.1 Calibration Rig

In order to accurately determine the performance of an air inlet, it is of paramount importance that the mass flow rate be measured as accurately as possible. Therefore, it is essential that the flow measuring cell be calibrated adequately.

Several methods to calibrate flow measuring cell can be used. As an example, many groups use a choked nozzle to calibrate their flow cell. However, the disadvantage of using choked nozzles resides in the fact that several nozzles are needed to completely calibrate the cell. Furthermore, when the cell is in series with the choked nozzle, the mass flow rate and the pressure ratio across the cell exit cannot be varied independently.

An alternate calibration method was developed to overcome these difficulties using the calibration cell shown in Fig. 10 [5].

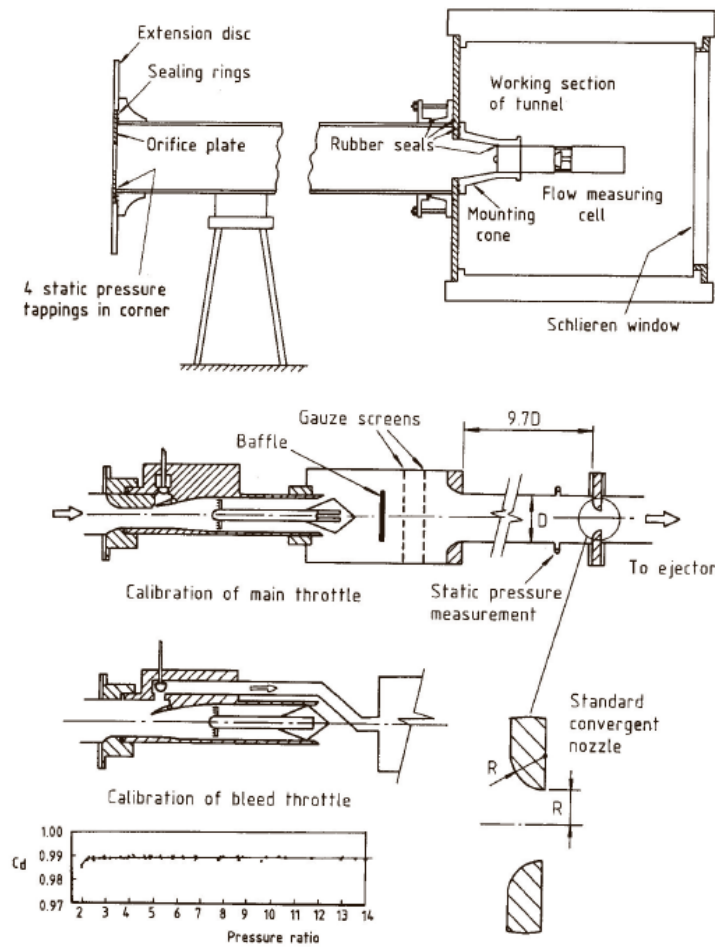


Figure 10: Flow cell calibration rig.

As seen in Fig. 10, the calibration rig is installed on the test section in place of one of the view port windows. The actual mass flow rate of air through the calibration rig is determined using a carefully machined and calibrated orifice plate. Alternatively, a calibrated bellmouth could be used at the inlet of the calibration rig instead of the orifice plate. The cell to be calibrated is mounted on the calibration rig so that its body stand in the wind tunnel test section. The contraction can also be replaced with a representation of the air intake flow path ahead of the measuring station.

In the DRDC Valcartier trisonic wind tunnel, a similar arrangement could be used. Instead of connecting the calibration apparatus to the section as described previously, it could be attached to a valve located on the exhausted reservoir as shown in Fig. 11 and 12. The difference in pressure between the reservoir and the atmospheric pressure in the lab would yield the required pressure

ratio across the calibration cell. The required pressure ratio is such that sonic flow is obtained at the valve throat. Theoretically, a minimum pressure ratio of about 2 between the upstream and downstream ends of the valve ensures sonic flow at the valve throat. Adjustment to the pressure ratio would be made by varying the conical valve position manually.

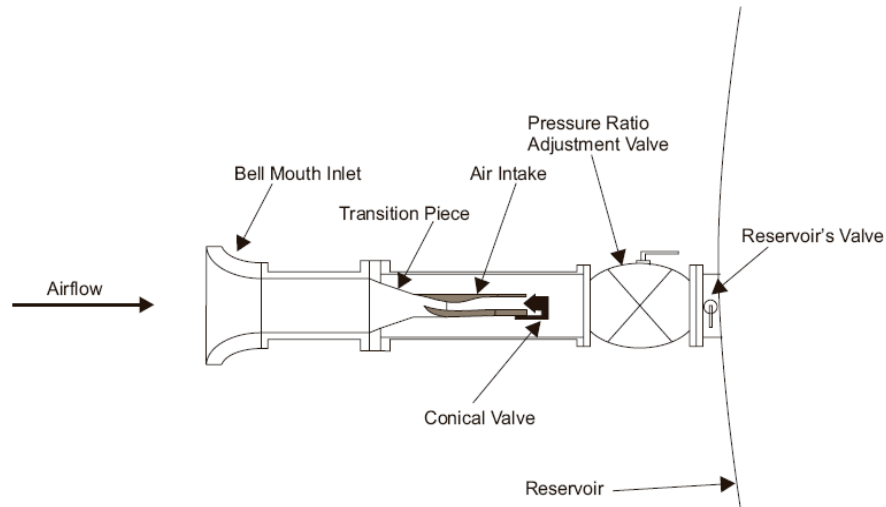


Figure 11: Flow cell calibration rig for DRDC Valcartier trisonic wind tunnel.

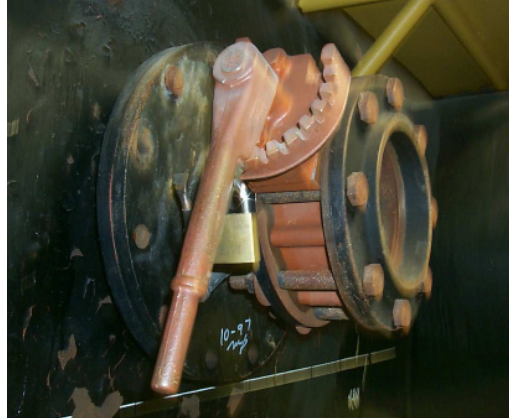


Figure 12: Valve on the wind tunnel reservoir.

Given the size of the reservoir, its pressure will probably remain unchanged during the calibration at a given operating point. This condition should be verified during real tests. Alternatively, the vacuum pump could be activated during the calibration so that a constant pressure could be maintained in the reservoir.

4.4.2 Discharge Coefficient

In order to calibrate the flow cell, the mass flow rate through the calibration rig must be determined accurately. This could be achieved with the use of a bellmouth or an orifice plate installed at the inlet of the calibration rig as shown in Fig. 10 and Fig. 11. The equation for the rate of flow of a fluid through an orifice plate is given by McGregor [4]. If a bellmouth is used, then referring to the notation in Fig. 13, the dimensionless mass flow rate can be calculated as

$$\frac{m_B \sqrt{T_{0\infty}}}{A_B \cdot P_{0\infty}} = C_B \sqrt{\frac{\gamma}{R}} \frac{M_B}{\left[1 + \frac{\gamma-1}{2} M_B^2\right]^{\frac{\gamma+1}{2(\gamma-1)}}} \quad (6)$$

In this equation, A_B is the minimum area of the bell mouth and M_B is the isentropic Mach number at that location obtained from

$$M_B = \sqrt{\frac{2}{\gamma-1} \left[\left(\frac{P_{0\infty}}{P_B} \right)^{\frac{\gamma-1}{\gamma}} - 1 \right]} \quad (7)$$

m_B is the mass flow rate through the bellmouth. The discharge coefficient C_B is required to account for the total pressure loss that occurs along the bellmouth wall. The discharge coefficient is usually supplied by the bellmouth manufacturer. It corresponds essentially to the ratio of the actual mass flow rate through the bellmouth and the calculated mass flow rate using Eq. 1.

Once the mass flow rate m_B through the calibration rig is determined accurately from a mass flow meter such as an orifice plate or a bellmouth, a discharge coefficient can be calculated for the conical valve. The discharge coefficient is given by

$$C_d = \frac{m_B \cdot c^*}{P_{0f} \cdot A_{e,geometric}} \quad (8)$$

Hence, the effective exit area $A_{e,effective}$ is given by

$$A_{e,effective} = C_d \cdot A_{e,geometric} \quad (9)$$

Thus, the flow ratio can be calculated using the following equation as mentioned previously by Eq. 2:

(10)

If this approach is favoured, then during the calibration process, a table of $A_{e, effective}$ versus valve position could be produced in order to determine the effective area during actual testing.

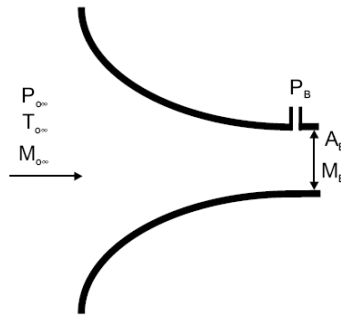


Figure 13: Bellmouth nomenclature.

4.5 Flow cell exit area calculation

The flow ratio A_∞ / A_c , when calculated using Eq. 7, is a function of the geometric exit area of the flow cell. Therefore, $A_{e,geometric}$ must be determined precisely as a function of the valve position. The nomenclature associated with the exit geometry of a flow cell with sharp edge is given in Fig. 14.

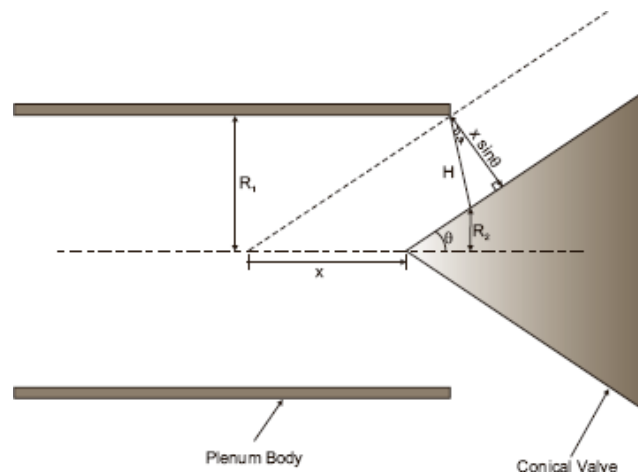


Figure 14: Nomenclature for the cell exit.

The geometric exit area corresponds to the minimum area of the conical surface generated by rotating the line H around the axis of the cell. For a given cone position x , the line H which yields the minimum exit area is obtained when the angle ψ equals 0 deg.

Referring to Fig. 14, the cone frustum area defined by the radii R_1 , R_2 and the slanted height H is given by

$$A_{e,geometric} = \pi.H(R_1 + R_2) \quad (11)$$

This equation can be rewritten in terms of the variables x and ψ as follows

$$A_{e,geometric} = \pi.\frac{x.\sin(\theta)}{\cos(\psi)}\left[2R_1 - \frac{x.\sin(\theta)}{\cos(\psi)}\cos(\theta - \psi)\right] \quad (12)$$

Thus, at a given conical valve x location, the minimum geometric area is given by

$$A_{e,geometric} = \pi.x.\sin(\theta)[2R_1 - x.\sin(\theta).\cos(\theta)] \quad (13)$$

In the case where a prismatic (wedge) valve is used instead of a conical valve, the geometric area is simply given by the following expression:

$$A_{e,geometric} = 2.x.w.\sin(\theta) \quad (14)$$

In this equation, w is the width of the air intake.

5 Total Pressure Recovery Measurements

The performance of an air intake can be evaluated by measuring the pressure recovery P_{02}/P_{00} . P_{02} is the total pressure at the engine face or at the combustor inlet whereas P_{00} is the free stream total pressure, as illustrated in Fig. 15..

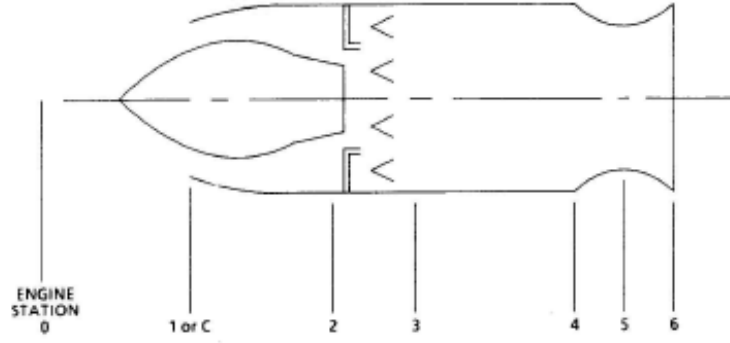


Figure 15: Ramjet engine schematic.

The higher the pressure recovery index the better is the inlet design. Furthermore, it can be shown that the pressure recovery contributes directly to the engine thrust level for which the dimensionless coefficient is given by the following expression:

$$C_F = \frac{2(A_6/A_R)}{\gamma_0 M_0^2} \left(\frac{\frac{P_{02}}{P_{00}} \cdot \frac{P_{04}}{P_{02}} \cdot n_N \left[\frac{P_6}{P_{06}} (1 + \gamma_6 M_6^2)_{ideal} \right]}{\frac{P_0}{P_{00}}} - 1 \right) - 2 \frac{A_0}{A_C} \frac{A_C}{A_R} \quad (15)$$

The air intake total pressure recovery (P_{02}/P_{00}) can be determined experimentally using Pitot tube rakes located at the engine face or at the subsonic diffuser end. Such total pressure measurements should be averaged somehow in order to define a unique value of the total pressure at the engine face or combustor inlet. Several averaging methods are available to achieve this goal. However, for air intake performance work, the entropy-flux mean and the area-weighted mean have been shown to be more suitable and practical.

The mean total pressure based on entropy flux is obtained from the following formula:

$$m_B \cdot \ln(\bar{P}_{02}) = \ln(P_{02}) dm \quad (16)$$

whereas the area weighted average is obtained from:

$$\bar{P}_{02} = \frac{1}{A_f} \int P dA \quad (17)$$

The area-average method is by far the most common method of calculating the total pressure from a Pitot tube rake. In the cases where it is decided that the total pressure will be area-averaged, it is common practice to manufacture the Pitot tube rake such that each tube is at the center of equivalent areas. In such case, the area-averaged total pressure is simply obtained by an arithmetic mean. McGregor [4] has shown that using Pitot tube rakes as those described previously, it was possible to evaluate to total pressure with an uncertainty of no more than $\pm 0.3\%$.

6 Air Intake Instrumentation

6.1 Surface Static Pressure Measurements

Detailed static pressure measurements should be made on the air intake surfaces in order to get a better picture of the flow physics associated with the internal flow. A longitudinal row of wall static-pressure orifices should extend from the leading edge of the air intake ramp down to the end of the subsonic diffuser. This will allow for a better evaluation of the subsonic diffuser performance. Furthermore, static pressure distributions are useful to locate shock impingement points as well as regions of flow separation. Finally, static pressure distributions are very helpful to validate numerical results.

In order to be able to locate the shock positions using surface static pressure, the taps density must be sufficiently high. On the other hand, the presence of a high number of static taps on a surface can modify the boundary layer thickness, trigger boundary layer transition and adversely affect the losses. Furthermore, static taps that are too closely spaced might yield erroneous pressure reading as they might feel the influence of adjacent holes. Therefore, a balance must be struck between the desire to maximize the number of taps and the need to avoid interference between the holes. Based on Roach & Turner [18] recommendation, the static taps should be spaced at least 50 diameters apart.

An additional row of static taps can also be added along the centerline of the cowl in the longitudinal direction. This can further help in locating the shock waves in the throat or subsonic diffuser region.

Static taps are also required to measure the static pressure at the Pitot rake location. In order to achieve that, an average static pressure can be measured by locating four (4) static taps at the center of each face in the Pitot tube rake plane. Using this average static pressure, the Mach number can be calculated using the total pressure measured with the Pitot tube.

An additional set of four static pressure measurements with taps distributed in a manner similar to those described previously can be located in the plenum between the Pitot tube rake and the conical valve.

When performing surface static pressure measurements an important parameter to be considered is the size of the holes. In order to maximize the number of static taps and avoid any aerodynamic interference between adjacent holes, one would like to minimize their size. However, there is a lower limit on the acceptable static taps size. This limit is imposed by the settling time required by the pressure measuring system to reach a constant pressure when subjected to a step change in test section pressure. For a pressure transducer, the pressure imbalance as a function of the time elapsed since the step change in pressure can be found as follows.

Assuming a fully-developed laminar flow in a long tube where the end effects are neglected, the axial velocity profile in the tube is given by Poiseuille's solution:

$$u_z = -\frac{1}{4\mu} \frac{\partial P}{\partial z} (R^2 - r^2) \quad (18)$$

The mass flow rate in the tube is then given by:

$$\frac{dm}{dt} = \rho u_z A = \frac{P}{R_g T} \int_0^R \left[\frac{1}{4\mu} \frac{\partial P}{\partial z} (R^2 - r^2) \right] 2\pi r dr \quad (19)$$

Integrating and simplifying, the following equation is obtained for the mass flow rate:

$$\frac{dm}{dt} = \frac{\pi d^4}{256 \mu L_e R_g T} (P^2 - P_1^2) \quad (20)$$

Taking the pressure to be changing isothermally, the mass flow rate can also be related to the change of pressure and volume as follows:

$$\frac{dm}{dt} = -\frac{d}{dt}(V\rho) = -\frac{1}{R_g T} \frac{d}{dt}(VP) = \frac{1}{R_g T} \left(-V \frac{dP}{dt} \right) \quad (21)$$

Equating the two expressions for the mass flow rate $\frac{dm}{dt}$

$$-V \frac{dP}{dt} = \frac{\pi d^4}{256 \mu L_e} (P^2 - P_1^2) \quad (22)$$

Separating variables and integrating using the fact that $P = P_o$ at $t = 0$

$$t = \frac{128 \mu L_e V_1}{\pi d^4 P_1} \ln \left[\frac{(P + P_1)(P_o - P_1)}{(P - P_1)(P_o + P_1)} \right] \quad (23)$$

This equation can be rewritten as

$$\frac{P - P_1}{P + P_1} = \frac{P_o - P_1}{P_o + P_1} e^{-t/\tau} \quad (24)$$

In this equation, P is the pressure at time t at the transducer face. P_0 is the initial pressure before the step change whereas the P_1 is the pressure afterward. The time constant τ is calculated as

$$\tau = \frac{128\mu.L_e.V_1}{\pi.d^4.P_1} \quad (25)$$

In this equation, V_1 is the volume of the entire system and d is the diameter of the static tap or probe orifice.

Very often the tubes connecting the pressure measurement point to the pressure transducer have various diameters. In order to simplify the calculations, it can be shown that a combination of tubes having different length and size can be replaced by an equivalent length L_e of tubing of diameter equal to that of the static taps or the probe orifice. The equivalent length is given by

$$L_e = L_1 + L_2 \left(\frac{d_1}{d_2} \right)^4 + L_3 \left(\frac{d_1}{d_3} \right)^4 + \dots \quad (26)$$

where L_1 and d_1 correspond to the dimensions of the static tap or the probe orifice.

From the above equations, the time required for the pressure error $\varepsilon = (P - P_1)/P_1$ to be reduced to an acceptable value can be estimated. This time will usually correspond to several time constants. Knowing that, proper holes and tube dimensions can be selected.

As example, if the wind tunnel is operated at a Mach number of 2.5, the test section pressure will be 5700 Pa and the air viscosity 9.19×10^{-6} N.s/m². Assuming that the tubing connecting the tap to the transducer has a diameter of 1/32 inch and a length of 1 meter, the system volume V_1 is found to be approximately 8.9×10^{-7} m³ neglecting the tap region volume. The equivalent length L_e can then be found to be equal to 0.015 meter assuming a tap diameter of 0.01 inch and a length of 5 mm together with the connecting tubing dimensions mentioned previously. Therefore, based on these values the time constant τ is found to be 0.12 sec. Considering 10 time constants, i.e. 0.005% threshold, this will translate in a settling time of about 1 sec which is a relatively long time. However, this is not a problem in the DRDC trisonic wind tunnel as the useful running time is at least four seconds.

6.2 Pitot Tube Rake

As mentioned in Section 5, a Pitot tube rake must be used in order to determine the total pressure profile at the engine face or at the end of the subsonic diffuser. This total pressure is used to calculate the pressure recovery, flow distortion and the mass flow rate. Examples of Pitot tube rakes can be seen in Figs. 16 and 17.

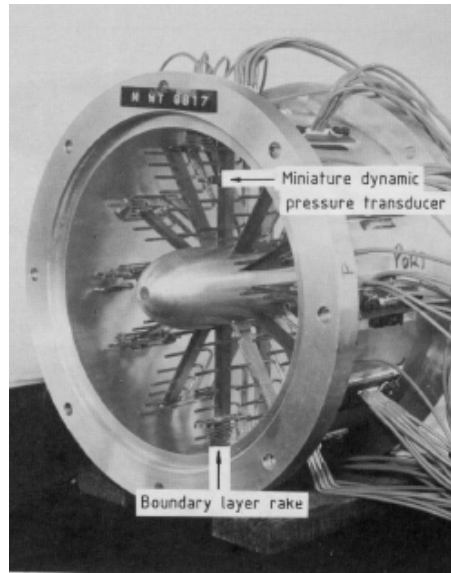


Figure 16: Pitot tube rake.

Alternatively, for test cases where the space is limited and Pitot tube rakes described previously cannot be accommodated, use of two-dimensional Pitot tube rakes might be more appropriate. Furthermore, in cases where a 2-D inlet is tested, the use of linear rakes eliminates the need for a transition piece from rectangular to circular cross-section. Such Pitot tube rakes were used by Borg [4]. He used 5 linear Pitot tube rakes having 5 tubes each thus forming a 2-D array of 5 by 5 probes. An isometric view of the Pitot tube used by Borg is shown in Fig. 17.

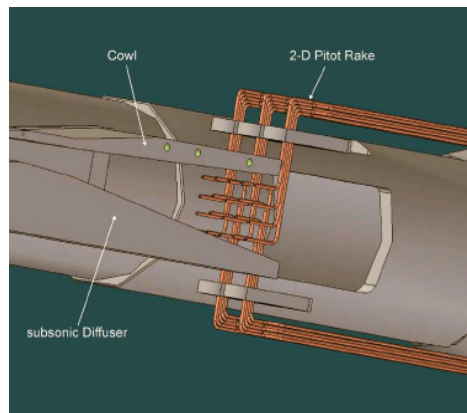


Figure 17: 2-D Pitot tube rakes.

Given that the size of the model that would be tested in the trisonic wind tunnel is very similar to that of Borg, it is foreseeable that a 2-D Pitot rake would be selected for tests at DRDC Valcartier. However, in order to increase the accuracy of the average total pressure measured at the diffuser end, the number of Pitot tube in the rake should be increased substantially. This

should be done without increasing the blockage significantly. Therefore, the diameter of the Pitot tubes should be reduced in order to limit the amount of extra blockage brought about by the additional number of probe used. The Pitot tubes used by Borg had an external diameter of 1 mm. As shown in the previous section, acceptable response times could still be obtained if Pitot tubes with a diameter of 0.5 mm were used. Hence, the number of tube in the rake could be easily double without unduly increasing the blockage.

6.3 Boundary Layer Control and Survey

In the DRDC Valcartier trisonic wind tunnel, the Reynolds number cannot be varied independently of the Mach number. Therefore, when tests are performed at high supersonic Mach numbers, the Reynolds number per unit length reaches relatively low values.

As an example, when the wind tunnel is operating at a Mach number of 2.5, the Reynolds number per unit length drops to 10.1×10^6 . Taking the VOLVO 2-D air inlet configuration which has an intake height of 19.69 mm, the Reynolds number is 198869. This is significantly below the critical Reynolds number for which transition occurs for a flat plate at a Mach number of 2.5. If tested in the DRDC wind tunnel, the model intake could probably be scaled by a factor of four given the size of the test section. This would yield a Reynolds number based on inlet height of 795476 which is still below the critical Reynolds number.

The presence of a low Reynolds number flow could have a significant impact on the performance of an air intake. At low Reynolds numbers, the boundary layer on the supersonic diffuser ramp surface will probably be laminar over a significant portion. However, a laminar boundary layer cannot withstand an adverse pressure gradient for an extended period of time before separating. Therefore, chances are that the boundary layer will separate, transition and re-attach on the compression surface thus forming a bridge across the compression surface as shown in Fig. 18.

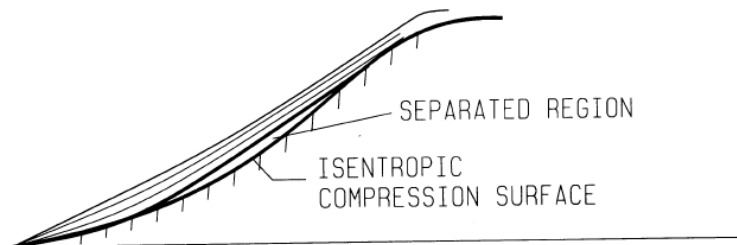


Figure 18: Boundary layer bridging across an isentropic ramp.

Bridging of the boundary layer across the compression ramp has a negative effect on the performance of the air intake as it reduces the amount of flow turning below that prescribed by the design. In the event that boundary layer separation on the compression ramp is found to be detrimental to the performance of the air intake corrective measures can be applied. Such measures include the use of boundary layer trip devices close to the ramp leading edge in order to force the boundary layer to transition to the turbulent state.

For the range of Mach numbers encountered in the wind tunnel, the boundary layer could be successfully tripped using wires or surface roughness such as sand. However, in order to succeed in causing boundary layer transition, the geometry of the trip device must be carefully selected. The trip device height must be such that it is approximately equal to that of the boundary layer. If the roughness height is too low, then the boundary layer won't be tripped. On the other hand, excessive trip device height would result in the formation of shocks that would cause total pressure losses. Therefore, it is necessary to predict or measure what the boundary layer height will be on the ramp prior to the actual tests.

In order to determine the height of the boundary layer on the compression ramp, the flow can be traversed in the direction normal to the surface using a Preston tube or a Pitot tube. The velocity profile can then be obtained near the surface and the boundary layer thickness determined. Alternatively, numerical prediction could be used to estimate the boundary layer thickness.

Boundary layer probe traverses can also be performed to assess the state of the boundary layer on the compression ramp. The velocity profile near the surface and the boundary layer shape factor can be calculated. Knowing the shape factor, the state of the boundary layer is easily deduced and thus a better understanding of the flow physics associated with the ramp flow is obtained.

The effect of boundary layer trip devices can then be monitored by performing boundary layer probe traverses. Provision for an access port to traverse the Preston tube in the direction normal to the surface would have to be made. Such configuration can be seen in Fig. 19.

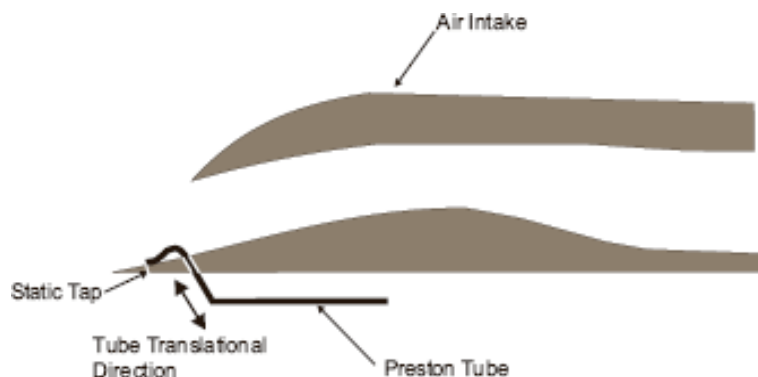


Figure 19: Boundary layer probe traverse set-up.

6.4 Oil Dot Visualization

A simple technique that can be used to detect a region of flow separation on a surface consists of applying an array of oil dots. Once the wind is turned on, the oil will spread more or less depending on the magnitude of the shear stress at the wall. Regions where separated flow is present are subjected to negligible shear stress. On the other hand, surfaces exposed to attached flow are subjected to shear stress with a principal component in the flow direction proportional to velocity gradient normal to the surface $\partial u / \partial y$. Therefore, in regions where higher shear stresses are present the oil will tend to spread more readily than in regions where the shear stresses are small such as under a separation bubble.

The main difficulty with this experimental technique consists in finding the right viscosity for the oil applied to the surface. The viscosity of the oil must be such that it spreads out sufficiently in regions of high shear stresses. Furthermore, the viscosity must be high enough for the oil streak to stay in place after the experiment to allow the experimentalist to take pictures.

Another problem that could be encountered in implementing this experimental technique could arise due to the passing of shock waves over the model surfaces when the wind tunnel flow is turned on and off. These shock waves tend to disturb the oil dots pattern at start-up and on shut down.

6.5 PIV Measurements

Particle Image Velocimetry (PIV) is an optical technique by which naturally occurring or seeded fine particles are illuminated, normally by a double pulsed laser, in a plane of the flow at least twice within a short and well known time interval. Two successive pictures of the particles lying in the light sheet are taken with a camera ideally located perpendicularly to the light sheet. The displacement of the particle over the time interval is determined by comparing the two pictures using appropriate algorithms. Modern algorithms also permit corrections for the case of the camera is not exactly perpendicular to the light sheet. A practical guide on using PIV technique is provided by Raffel et al [10].

Besides the difficulty of flow seeding and integration of the optics inside the wind tunnel test section, another issue in trying to implement this experimental technique resides in the need to properly light up the region of interest with the laser light sheet. One possibility would consist in installing the laser and the required lens in the wind tunnel upstream of the throat as shown in Fig. 20.

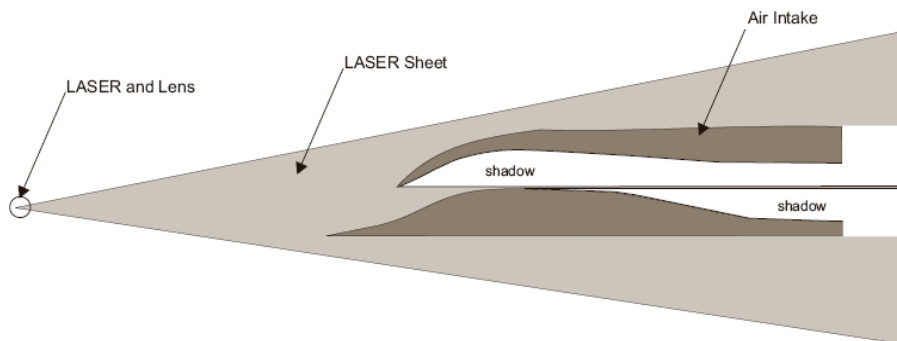


Figure 20: PIV set-up for air intake tests.

This setup would illuminate the external compression ramp. However, because of the presence of the cowl, practically no illumination of the flow inside the air intake would result. An alternative to this setup would be to incorporate a slot along the longitudinal axis of the compression ramp or the cowl. This slot would be filled with an optically clear material to allow the laser light sheet to illuminate the flow within the intake from the top or the bottom.

The PIV method is by far the technique that would required the most experimentation before actual measurements can be performed on an air intake model.

6.6 Schlieren Technique

Schlieren is an optical technique used to observe phenomena invisible to the human eye, where density gradients in media of interest are present. The technique is largely used in compressible fluid dynamics, permitting visualisation of shock and expansion wave structures, boundary layer separation, etc. In this case, the technique takes advantage of the variation in the refractive properties of light presented in compressible flows, to visualize particular features of interest. When coupled to high speed cameras the technique could permit the observation of those phenomena at near real time.

Depending of the optics being used, the technique can be classified as lens or mirror systems. The latest systems have the best trade-off between field-of-view and cost [11]. In mirror systems, parabolic and spherical mirrors are largely used. Despite their higher prices, parabolic mirrors are the common choice in installations where high resolution is the most important parameter to be considered since spherical mirrors have the intrinsic disadvantage of creating aberration.

The method permits different configurations to comply with specific application and sensitivity requirements as well as space constraints. The most commonly used Schlieren set-ups are the so-called Z-type presented in Fig. 21.

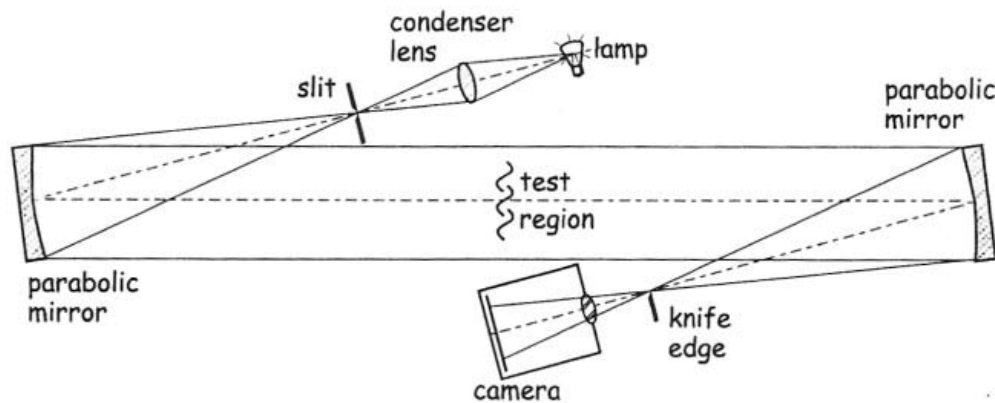


Figure 21: Typical Schlieren arrangement – The Z-Type 2-mirrors.

However, to increase the sensitivity of Schlieren system, other configurations have been commonly used in the experiments, such as the single-mirror coincident system presented in Fig. 22. Another advantage of this arrangement is the smaller space required for its set-up. Further discussion on Schlieren technique is presented in Settles [11].

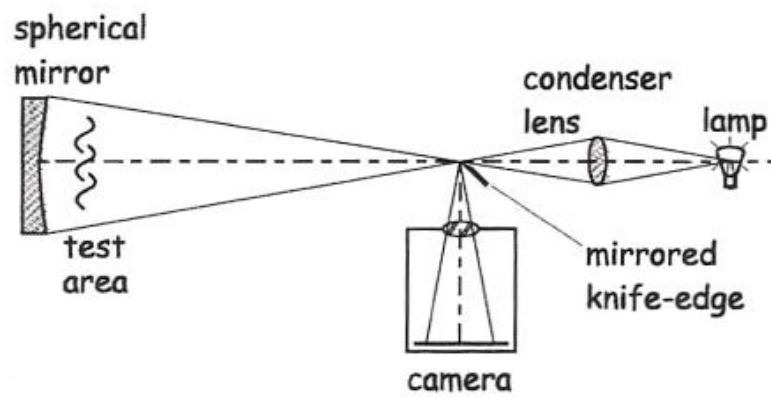


Figure 22: Typical Schlieren arrangement – Single mirror coincident system.

7 Tentative Test Matrix

In this section, a wind tunnel test campaign to obtain a large database of the air intake performance parameters is presented. Different Mach numbers, AoA of the model, boundary layer bleed position, and backpressures are considered.

Table 1: Field Definitions.

FIELD NUMBER	DESCRIPTION
Field 1: Model definition	VOLVO
Field 2: Mach number	20: 2.0; 25: 2.5; 30: 3.0
Field 3: Prismatic valve position	1: 30.57mm, 2: 29.57mm, 3: 28.57mm, 4: 26.57mm, 5: 23.57mm, 6: 20.57mm, 7: 18.57mm, 8: 16.57mm, 9: 14.57mm
Field 4: Angle of attack (AoA)	(25): -2.5°, 0: 0°, 5: 5°, 10: 10°
Field 5: Bleed insert opening	0: Closed, 50: 5.0 mm
Field 6: Repetition of a run *	1, 2, .../blank: original configuration

Table 2: Test Matrix – Mach Number 2.5.

Model	Mach number	Prismatic valve position	AoA	Bleed insert	Repeat
VOLVO	2.0	1	0	5.0 mm	1,2,...
VOLVO	2.0	2	0	5.0 mm	1,2,...
VOLVO	2.0	3	0	5.0 mm	1,2,...
VOLVO	2.0	4	0	5.0 mm	1,2,...
VOLVO	2.0	5	0	5.0 mm	1,2,...
VOLVO	2.0	1	-2.5	5.0 mm	1,2,...
VOLVO	2.0	2	-2.5	5.0 mm	1,2,...
VOLVO	2.0	3	-2.5	5.0 mm	1,2,...
VOLVO	2.0	4	-2.5	5.0 mm	1,2,...
VOLVO	2.0	5	-2.5	5.0 mm	1,2,...
VOLVO	2.0	1	5	5.0 mm	1,2,...
VOLVO	2.0	2	5	5.0 mm	1,2,...
VOLVO	2.0	3	5	5.0 mm	1,2,...
VOLVO	2.0	4	5	5.0 mm	1,2,...
VOLVO	2.0	5	5	5.0 mm	1,2,...
VOLVO	2.0	1	10	5.0 mm	1,2,...
VOLVO	2.0	2	10	5.0 mm	1,2,...
VOLVO	2.0	3	10	5.0 mm	1,2,...
VOLVO	2.0	4	10	5.0 mm	1,2,...
VOLVO	2.0	5	10	5.0 mm	1,2,...
VOLVO	2.0	1	15	5.0 mm	1,2,...
VOLVO	2.0	2	15	5.0 mm	1,2,...
VOLVO	2.0	3	15	5.0 mm	1,2,...
VOLVO	2.0	4	15	5.0 mm	1,2,...
VOLVO	2.0	5	15	5.0 mm	1,2,...

Table 3: Test Matrix – Mach Number 2.5.

Model	Mach number	Prismatic valve position	AoA	Bleed insert	Repeat
VOLVO	2.5	1	0	5.0 mm	1,2,...
VOLVO	2.5	2	0	5.0 mm	1,2,...
VOLVO	2.5	3	0	5.0 mm	1,2,...
VOLVO	2.5	4	0	5.0 mm	1,2,...
VOLVO	2.5	5	0	5.0 mm	1,2,...
VOLVO	2.5	1	-2.5	5.0 mm	1,2,...
VOLVO	2.5	2	-2.5	5.0 mm	1,2,...
VOLVO	2.5	3	-2.5	5.0 mm	1,2,...
VOLVO	2.5	4	-2.5	5.0 mm	1,2,...
VOLVO	2.5	5	-2.5	5.0 mm	1,2,...
VOLVO	2.5	1	5	5.0 mm	1,2,...
VOLVO	2.5	2	5	5.0 mm	1,2,...
VOLVO	2.5	3	5	5.0 mm	1,2,...
VOLVO	2.5	4	5	5.0 mm	1,2,...
VOLVO	2.5	5	5	5.0 mm	1,2,...
VOLVO	2.5	1	10	5.0 mm	1,2,...
VOLVO	2.5	2	10	5.0 mm	1,2,...
VOLVO	2.5	3	10	5.0 mm	1,2,...
VOLVO	2.5	4	10	5.0 mm	1,2,...
VOLVO	2.5	5	10	5.0 mm	1,2,...
VOLVO	2.5	1	15	5.0 mm	1,2,...
VOLVO	2.5	2	15	5.0 mm	1,2,...
VOLVO	2.5	3	15	5.0 mm	1,2,...
VOLVO	2.5	4	15	5.0 mm	1,2,...
VOLVO	2.5	5	15	5.0 mm	1,2,...

Table 4: Test Matrix – Mach Number 3.0.

Model	Mach number	Prismatic valve position	AoA	Bleed insert	Repeat
VOLVO	3.0	1	0	5.0 mm	1,2,...
VOLVO	3.0	2	0	5.0 mm	1,2,...
VOLVO	3.0	3	0	5.0 mm	1,2,...
VOLVO	3.0	4	0	5.0 mm	1,2,...
VOLVO	3.0	5	0	5.0 mm	1,2,...
VOLVO	3.0	1	-2.5	5.0 mm	1,2,...
VOLVO	3.0	2	-2.5	5.0 mm	1,2,...
VOLVO	3.0	3	-2.5	5.0 mm	1,2,...
VOLVO	3.0	4	-2.5	5.0 mm	1,2,...
VOLVO	3.0	5	-2.5	5.0 mm	1,2,...
VOLVO	3.0	1	5	5.0 mm	1,2,...
VOLVO	3.0	2	5	5.0 mm	1,2,...
VOLVO	3.0	3	5	5.0 mm	1,2,...
VOLVO	3.0	4	5	5.0 mm	1,2,...
VOLVO	3.0	5	5	5.0 mm	1,2,...
VOLVO	3.0	1	10	5.0 mm	1,2,...
VOLVO	3.0	2	10	5.0 mm	1,2,...
VOLVO	3.0	3	10	5.0 mm	1,2,...
VOLVO	3.0	4	10	5.0 mm	1,2,...
VOLVO	3.0	5	10	5.0 mm	1,2,...
VOLVO	3.0	1	15	5.0 mm	1,2,...
VOLVO	3.0	2	15	5.0 mm	1,2,...
VOLVO	3.0	3	15	5.0 mm	1,2,...
VOLVO	3.0	4	15	5.0 mm	1,2,...
VOLVO	3.0	5	15	5.0 mm	1,2,...

8 Conclusion

An increasing interest in ramjet propulsion for tactical supersonic missiles has been observed worldwide recently, due to the improved performance it provides in terms of range and speed compared to solid propellant rocket propulsion. DRDC Valcartier in Canada and TNO Defence, Security and Safety in the Netherlands are currently working jointly to improve their capacity to numerically predict the internal performance of ramjet powered missiles.

A meticulous survey of the open literature on supersonic air intakes revealed that the amount of data available to properly validate performance prediction codes applied to ramjet engines is very limited. A series of reports from Volvo Flygmotor AB concerning 2-D air inlets on cruise missiles using ramjet airbreathing propulsion were considered the most suitable for our studies. The reports present several results on different configurations of 2-D supersonic air inlets both in isolation and mounted on a missile body, as well as detailed drawings for the construction of a wind tunnel model. For the tests at DRDC Valcartier, the research efforts will focus on the main air intake performance parameters. The air intake will be studied in isolation in order to eliminate the complexities related to the influence of the missile forebody.

The Volvo reports include data on the air intake performance parameters, such as pressure recovery and mass flow rate measurements as a function of Mach number, AoA and intake backpressure. Pressure recovery data are also presented for various bleed flow rates. For the DRDC Valcartier trisonic wind tunnel experiments, static pressure taps along the compression surface or the cowl could gather more information on flow physics. This data was not gathered in the Volvo tests. Furthermore, no flow visualization techniques such as Schlieren photography, PIV or oil dots were presented by Volvo. These techniques could be considered during the test campaign at DRDC Valcartier to help in identifying shock locations and boundary layer separation. This data is necessary for numerical validation and would complement the database from the Volvo experiments.

The use of a larger model could result in a higher Reynolds number based on inlet height. This is highly desirable, as the DRDC wind tunnel operates at very low pressures and the resulting Reynolds numbers per unit length are relatively small. Our choice for the size of the air intake test model would be twice the size of the Volvo air intake.

To simulate the effect of a combustor and to obtain the desired backpressure, a device to vary internal flow pressure in the model is required. This device should be located at some length downstream of the subsonic diffuser and be aligned with the inlet longitudinal axis. For testing air intakes in the DRDC Valcartier trisonic wind tunnel, a manually operated prismatic valve for intake backpressure control would be the best alternative to minimize complexity and allow integration of the model to the wind tunnel test section.

For mass flow rate measurements, a mass flow meter is not recommended due to its large size. The other two flow measurement techniques, namely the choked valve technique and the duct-based mass flow rate estimation technique, have their disadvantages as well. Both estimation techniques require an accurate estimation of the total pressure in the duct downstream of the subsonic diffuser. Since the model will be instrumented with static pressure taps just upstream of the total pressure rake, total and static pressure measurements will be available to evaluate both

mass flow rate estimation techniques. However, pressure measurements should be very precise, because when differences between total and static pressures are small, even small inaccuracies in the pressure measurements may cause unacceptable inaccuracies in the calculated values of the duct Mach number and therefore induce errors in the estimation of the captured mass flow rate by the intake. The choked valve mass flow rate estimation technique needs calibration beforehand in order to determine the effective valve throat area as a function of wedge insert depth and bleed insert position.

9 References

- [1] Mayer, A.E.H.J, Halswijk, W. H. C., Konduur, H. J., Lauzon, M., Stowe, R., A modular ducted rocket missile for threat and performance assessment, *AIAA Modeling and Simulation Technologies Conference and Exhibit*, 15-18 Aug. 2005, San Francisco, California, AIAA 2005-6013.
- [2] Johansson, U., Investigation of inlets with a rear mounted airbreathing engine, Volvo Flygmotor Aerodynamics, doc. nr. LA 202, March 1992.
- [3] Moerel, J.-L., Lesage, F., Hamel, N., Corriveau, D., “Aerodynamic model improvement for airbreathing missiles – Selection of reference configurations”, DRDC TM 2004-444, February 2006.
- [4] Borg, R., Investigation of inlet installed performance with a twin cheek inlet installation on a missile, Volvo Flygmotor Aerodynamics, doc.nr. 9370-759, December 1993.
- [5] Seddon, J., Goldsmith, E. L., Intake Aerodynamics, AIAA Education Series, 1985.
- [6] Mahoney, J.J., Inlets for Supersonic Missiles, AIAA Education Series, 1990.
- [7] McGregor, I, “The characteristics and calibration of two types of airflow metering device for investigating the performance pf model air-intakes”, Royal Aircraft Establishment, Technical Report 71212, Novembre 1971.
- [8] Woollett, R. R., Connors, J. F., “Zero-angle-of-attack performance of two-dimensional inlets near Mach number 3”, NACA Research Memorandum RM E55K01, February 1956.
- [9] Sinclair, A. R., Robins, A.W, “A method for the determination of the time lag in pressure measuring systems incorporating capillaries”, NACA Technical Note 2793, September 1952.
- [10] Raffel, M., Willert, C., Kompenhans, J., Particle Image Velocimetry, Springer-Verlag Berlin Heidelberg, 1998.
- [11] Settles, G. S., Schlieren and Shadowgraph Techniques, Visualizing Phenomena in Transparent Media, Springer-Verlang, 2001.
- [12] Brown, C. S., Goldsmith, E. L., “Measurement of the internal performance of a rectangular air intake mounted on a fuselage at Mach numbers from 1.6 to 2”, Part V, Royal Aircraft Establishment, Technical Report 72136, September 1972.
- [13] Borg, R., Development and wind tunnel tests on isolated 2D-inlets with relatively high design Mach number 2.75, 2nd phase, Volvo Flygmotor Aerodynamics, doc. nr. LA 185, January 1989.

- [14] Johansson, U., Development and wind tunnel tests on isolated 2D-inlets with a design Mach number of 2.5, Volvo Flygmotor Aerodynamics, doc. nr. LA 197 I, November 1989.
- [15] Johansson, U., Development and wind tunnel tests on isolated 2D-inlets with a design Mach number of 2.5, Volvo Flygmotor Aerodynamics, doc. nr. LA 197 II, November 1989.
- [16] Borg, R., Investigation of inlet installed performance with a single underslung installation on a missile forebody. Inlet design Mach number 2.75, Volvo Flygmotor Aerodynamics, doc. nr. LA 201, December 1991.
- [17] Johansson, U., Investigation of inlets for ramjet applications. Wind tunnel test on 2-D inlet VI, bypass type, Volvo Flygmotor Aerodynamics, doc. nr. 9370-754, February 1993.
- [18] Roach, P. E., Turner, J. T., Premature Boundary Layer Transition Caused by Surface Static Pressure Tappings, *Aeronautical Journal*, February 1988.

List of symbols/abbreviations/acronyms/initialisms

A	Area, m ²
AoA	Angle of attack, deg
CFD	Computational Fluid Dynamics
C_B	Discharge coefficient
DND	Department of National Defence
DRDC	Defence Research & Development Canada
DRDKIM	Director Research and Development Knowledge and Information Management
m	Mass flow rate, kg/s
M	Mach number
P_0	Total pressure, Pa
PIV	Particle Image Velocimetry
R	Gas constant, 287 J/kg.K for air
Re	Reynolds number
R&D	Research & Development
T_0	Total temperature, K
γ	Ratio of specific heats, 1.4 for air
π	Pressure recovery

This page intentionally left blank.

Distribution list

Document No.: DRDC TM 2008-116

LIST PART 1: Internal Distribution by Centre

- 1 DG
- 1 H/Precision Weapons Section
- 3 Document Library
- 1 D. Corriveau (author)
- 1 R. Pimentel (author)
- 1 F. Lesage
- 1 N. Hamel
- 1 F. Wong
- 1 R. Stowe
- 1 R. Farinaccio
- 1 M. Lauzon

13 TOTAL LIST PART 1

LIST PART 2: External Distribution by DRDKIM

- 1 Library and Archives Canada
- 1 DRDKIM (PDF file)
- 1 J.-L. Moerel
TNO Defence Security and Safety
P.O. Box 45, 2280AA Rijswijk
The Netherlands

3 TOTAL LIST PART 2

16 TOTAL COPIES REQUIRED

This page intentionally left blank.

DOCUMENT CONTROL DATA		
(Security classification of title, body of abstract and indexing annotation must be entered when the overall document is classified)		
1. ORIGINATOR (The name and address of the organization preparing the document. Organizations for whom the document was prepared, e.g. Centre sponsoring a contractor's report, or tasking agency, are entered in section 8.) Defence R&D Canada – Valcartier 2459 Pie-XI Blvd North Quebec (Quebec) G3J 1X5 Canada	2. SECURITY CLASSIFICATION (Overall security classification of the document including special warning terms if applicable.) <u>UNCLASSIFIED</u>	
3. TITLE (The complete document title as indicated on the title page. Its classification should be indicated by the appropriate abbreviation (S, C or U) in parentheses after the title.) Wind tunnel tests on two-dimensional air intakes at DRDC Valcartier (U)		
4. AUTHORS (last name, followed by initials – ranks, titles, etc. not to be used) Corriveau, D., Pimentel, R.		
5. DATE OF PUBLICATION (Month and year of publication of document.) April 2009	6a. NO. OF PAGES (Total containing information, including Annexes, Appendices, etc.) 52	6b. NO. OF REFS (Total cited in document.) 18
7. DESCRIPTIVE NOTES (The category of the document, e.g. technical report, technical note or memorandum. If appropriate, enter the type of report, e.g. interim, progress, summary, annual or final. Give the inclusive dates when a specific reporting period is covered.) Technical Memorandum		
8. SPONSORING ACTIVITY (The name of the department project office or laboratory sponsoring the research and development – include address.)		
9a. PROJECT OR GRANT NO. (If appropriate, the applicable research and development project or grant number under which the document was written. Please specify whether project or grant.) 13eg12	9b. CONTRACT NO. (If appropriate, the applicable number under which the document was written.)	
10a. ORIGINATOR'S DOCUMENT NUMBER (The official document number by which the document is identified by the originating activity. This number must be unique to this document.) DRDC Valcartier TM 2008-116	10b. OTHER DOCUMENT NO(s). (Any other numbers which may be assigned this document either by the originator or by the sponsor.) N/A	
11. DOCUMENT AVAILABILITY (Any limitations on further dissemination of the document, other than those imposed by security classification.) Unlimited		
12. DOCUMENT ANNOUNCEMENT (Any limitation to the bibliographic announcement of this document. This will normally correspond to the Document Availability (11). However, where further distribution (beyond the audience specified in (11) is possible, a wider announcement audience may be selected.) Unlimited		

13. **ABSTRACT** (A brief and factual summary of the document. It may also appear elsewhere in the body of the document itself. It is highly desirable that the abstract of classified documents be unclassified. Each paragraph of the abstract shall begin with an indication of the security classification of the information in the paragraph (unless the document itself is unclassified) represented as (S), (C), (R), or (U). It is not necessary to include here abstracts in both official languages unless the text is bilingual.)

An increasing interest in ramjet propulsion for tactical supersonic missiles has been observed worldwide recently, due to the improved performance it provides in terms of range, speed and manoeuvrability compared to solid propellant rocket propulsion. DRDC Valcartier in Canada and TNO Defence, Security and Safety in the Netherlands are currently working jointly to improve their capacity to numerically predict the internal performance of ramjet powered missiles. Air intakes are employed on several operational cruise missiles that use ramjet airbreathing propulsion during the supersonic cruise flight phase. It is recognized that operation of airbreathing missiles is strongly dependent on the efficiency of their air intake systems.

Accurate experimental data on the performance parameters of ramjet air intakes at different angles of attack during on and off-design operations are required in order to verify the accuracy of the numerical predictions. However, the amount and quality of experimental data on air intake performance available in the open literature is fairly limited. Therefore, it was decided to investigate the possibility of performing air intake performance measurements in the trisonic wind tunnel at DRDC Valcartier to generate additional experimental data for comparison with numerical simulations.

This report describes possible procedures and instrumentation that would be required to perform eventual wind tunnel tests on ramjet air intakes in the DRDC Valcartier trisonic wind tunnel.

On observe dans le monde une augmentation d'intérêt envers les statoréacteurs pour la propulsion des missiles supersoniques, à cause de ses meilleures performances sur la portée, vitesse et manoeuvrabilité comparativement à la propulsion avec des propergols solides. RDDC Valcartier au Canada et TNO Defence, Security and Safety aux Pays-Bas présentent travaillent conjointement afin d'améliorer leur capacité à prédire numériquement la performance des statoréacteurs. Les entrées d'air sont utilisées pour divers missiles de croisière avec propulsion à l'aspiration d'air pendant la phase de vol supersonique.

Des données précises sur la performance des prises d'air pour statoréacteurs sont requises à angle d'attaque et en condition hors opération afin de vérifier la précision des prédictions numériques. Cependant, la quantité et la qualité des données expérimentales sur les prises d'air disponible dans la littérature ouverte sont assez limitées. Dons, il a été décidé de regarder la possibilité d'effectuer des mesures de performance des prises d'air dans la soufflerie trisonique du RDDC Valcartier de manière à générer des données expérimentales additionnelles pour fin de comparaison avec les simulations numériques.

Ce rapport présent décrit possibles procédures et l'instrumentation nécessaires pour la réalisation des éventuels essais, à la soufflerie trisonique de RDDC Valcartier, sur les entrées d'air pour les statoréacteurs.

14. **KEYWORDS, DESCRIPTORS or IDENTIFIERS** (Technically meaningful terms or short phrases that characterize a document and could be helpful in cataloguing the document. They should be selected so that no security classification is required. Identifiers, such as equipment model designation, trade name, military project code name, geographic location may also be included. If possible keywords should be selected from a published thesaurus, e.g. Thesaurus of Engineering and Scientific Terms (TEST) and that thesaurus identified. If it is not possible to select indexing terms which are Unclassified, the classification of each should be indicated as with the title.)

inlets

intake

missile

airbreathing

wind tunnel

internal aerodynamics

ramjet

missile performance

Defence R&D Canada

Canada's Leader in Defence
and National Security
Science and Technology

R & D pour la défense Canada

Chef de file au Canada en matière
de science et de technologie pour
la défense et la sécurité nationale



www.drdc-rddc.gc.ca

